IOP Publishing Journal of Neural Engineering
J. Neural Eng. 12 (2015) 046003 (9pp) doi:10.1088/1741-2560/12/4/046003

A novel lead design enables selective deep brain stimulation of neural populations in the subthalamic region

Kees J van Dijk[1], Rens Verhagen[2], Ashutosh Chaturvedi[3], Cameron C McIntyre[3], Lo J Bour[2], Ciska Heida[1] and Peter H Veltink[1]

[1] MIRA institute for Biomedical Engineering and Technical Medicine, University of Twente, Enschede, NL, The Netherlands
[2] Department of Neurology/Clinical Neurophysiology, Academic Medical Center, Amsterdam, NL, The Netherlands
[3] Department of Biomedical Engineering, Case Western Reserve University, Cleveland, OH, USA

E-mail: k.j.vandijk@utwente.nl

Received 20 October 2014, revised 31 March 2015
Accepted for publication 22 April 2015
Published 28 May 2015

Abstract

Objective. The clinical effects of deep brain stimulation (DBS) of the subthalamic nucleus (STN-DBS) as a treatment for Parkinson's disease are sensitive to the location of the DBS lead within the STN. New high density (HD) lead designs have been created which are hypothesized to provide additional degrees of freedom in shaping the stimulating electric field. The objective of this study is to compare the performances of a new HD lead with a conventional cylindrical contact (CC) lead. *Approach.* A computational model, consisting of a finite element electric field model combined with multi-compartment neuron and axon models representing different neural populations in the subthalamic region, was used to evaluate the two leads. We compared ring-mode and steering-mode stimulation with the HD lead to single contact stimulation with the CC lead. These stimulation modes were tested for the lead: (1) positioned in the centroid of the STN, (2) shifted 1 mm towards the internal capsule (IC), and (3) shifted 2 mm towards the IC. Under these conditions, we quantified the number of STN neurons that were activated without activating IC fibers, which are known to cause side-effects. *Main results.* The modeling results show that the HD lead is able to mimic the stimulation effect of the CC lead. Additionally, in steering-mode stimulation there was a significant increase of activated STN neurons compared to the CC mode. *Significance.* From the model simulations we conclude that the HD lead in steering-mode with optimized stimulation parameter selection can stimulate more STN cells. Next, the clinical impact of the increased number of activated STN cells should be tested and balanced across the increased complexity of identifying the optimized stimulation parameter settings for the HD lead.

Keywords: deep brain stimulation, Parkinson's disease, computational modeling, steering-mode stimulation, novel lead design

(Some figures may appear in colour only in the online journal)

Introduction

Deep brain stimulation (DBS) for Parkinson's disease (PD) patients may reduce considerably their symptoms including tremor, rigidity and akinesia [1, 2]. The clinical procedure involves the implantation of a DBS lead, consisting of multiple electrode contacts, through which continuous high frequency electric pulses (typically with a frequency of 130 Hz and pulse duration of 60–90 μs) are delivered in a specific brain area [3]. In the case of PD, the preferred targeted brain

area is the subthalamic nucleus (STN) [4–6]. This nucleus is a small biconvex shaped structure located deep in the brain and is surrounded by several bundles of myelinated fibers such as the lenticular fasciculus, and internal capsule (IC) [7]. The clinical outcome of the therapy is rather sensitive to the precise location of the DBS lead within the STN [8, 9]. Unfortunately, despite careful stereotactic planning with high-tech 3D MRI imaging techniques, placement errors within a range from 1 to 3 mm still may occur [10, 11]. Also, a DBS lead which initially was placed correctly post-surgery may become displaced over time due to several reasons [12, 13].

In case of a displaced lead, the injected stimulation current will spread out to unwanted brain regions and, for instance, may evoke activation in the easily excitable myelinated fibers passing nearby [14]. Activation of some of these myelinated fiber tracts may have a positive clinical effect, as is the case for the efferent globus pallidus internus (GPi) fibers in the lenticular fasciculus [15], or the motor cortex axons of the hyperdirect pathway [16]. However, both activation of fibers in the IC as well as neurons in the non-sensorimotor part of the STN may cause undesirable side-effects including ocular deviation, speech difficulties, facial contractions, a decline in cognitive functioning, and mood changes, [9, 17–21]. Given these side-effects, it is crucial to prevent unwanted current spread and ultimately to be able to compensate for a displacement without the need to reposition the DBS lead.

To compensate for positioning errors, the stimulating electric field can be adjusted by selecting the appropriate electrode contact(s) on the lead. In this manner, the conventional lead, consisting of four cylindrical contacts (CCs), is able to compensate for a displacement primarily in the dorsal–ventral direction. New lead designs are currently in development, which additionally enable steering of the stimulating field in the lateral–medial and anterior–posterior directions through a high-density (HD) array of contacts [22, 23]. An example of this type is the HD lead in development at Sapiens Steering Brain Stimulation BV (Eindhoven, NL), which is currently in a clinical test phase [24]. The latest design of this HD lead, will consist of ten rows along the lead and each row containing four individual oval shaped electrode contacts, facing different directions (figure 2). With this design, the spatial steering of the stimulation field is achieved by activation of an appropriate combination of the 40 available contacts. Unfortunately, the high amount of possible combinations of contacts will increasingly complicate selecting optimal stimulation parameters. Therefore, more insight is needed into the spatial steering-modes of HD leads and new tools need to be developed to find these optimal steering parameters.

Computational models can be used to evaluate and visualize steering-modes DBS effects in the brain [22, 25, 26]. For example, Martens *et al* (2010) evaluated a prototype design of a HD lead using a computational model. In their model, they showed that the HD lead is able to spatially steer the electric field in a homogeneous isotropic volume conductor and shift the center of the volume of activated tissue. This result suggests that indeed it is possible to compensate for lead displacement using an HD lead. However, as they also noted in their discussion, calculations were performed under the assumption that the brain acts as a homogenous isotropic volume conductor. In general, the state of the art electric field models with heterogeneous anisotropic volume conduction show significant differences in the shape of their reconstructed electric fields compared to the homogeneous isotropic models [14, 27–29]. To evaluate the possibility to compensate for a lead displacement, the effect of the steered field on the various neural populations in the subthalamic region needs to be estimated. The activation effect is often estimated by the volume of tissue activated, i.e. the tissue enclosed within an iso-surface of the activation function [30, 31]. However, a more realistic approach, with respect to the surrounding axon fiber bundles, is to evaluate the stimulation effect in more detailed multi-compartment neuron models of different neural populations in the subthalamic region [28].

In this study, we used computational models to investigate the stimulation effect of a HD lead and its ability to compensate for a lead displacement. The model system, based on a previous study by Chaturvedi *et al* [32], included a heterogeneous anisotropic volume conductor with multi-compartment neuron and axon models of three important neural populations in the subthalamic region [32]. Two populations, i.e., the STN projections cells and the efferent GPi fibers in lenticular fasciculus, represent therapeutic DBS targets while a third population, i.e., the IC fibers, represents a neural population that will cause side-effects when stimulated. In the current model we have compared the stimulation effect of the conventional CC lead with that of a HD lead, which has 40 contacts. The aim of the computer simulation was to initiate an action potential in a maximum percentage of STN cells without activating IC fibers. Simulations were performed with the DBS leads positioned at three different locations within the STN, using multiple stimulation modes.

Materials and methods

The subthalamic region

In the current study, the computational model of the subthalamic region was based on previous work of Chaturvedi *et al* [32]. In summary, their model system consists of two parts; the electric field model, and the neuron model. The electric field model is a finite element method (FEM) model with the geometry and volume conduction properties of the subthalamic region based on a human brain atlas, which consists of a T1 MRI and a diffusion tensor imaging (DTI) dataset [33]. The DTI dataset was used to estimate the anisotropy and heterogeneity of the tissue conductivity in the brain [34]. The model incorporated a 0.5 mm tissue encapsulation layer around the electrode to account for the chronic electrode impedance of around 1 kΩ for the CC lead. A multiresolution finite element mesh was used with over 4.2 million nodes. In this FEM model the Poisson equation was solved in three-dimensions to determine the potential field

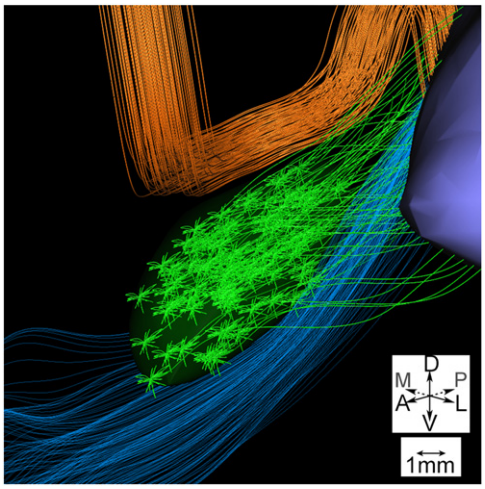

Figure 1. The anatomical model of the subthalamic region viewed from anterior–lateral direction. Two relevant nuclei are shown: the STN (green volume), and the globus pallidus (purple volume). The three neural populations are shown: the efferent GPi fibers (orange), the IC fibers (blue) and the STN projection neurons (green).

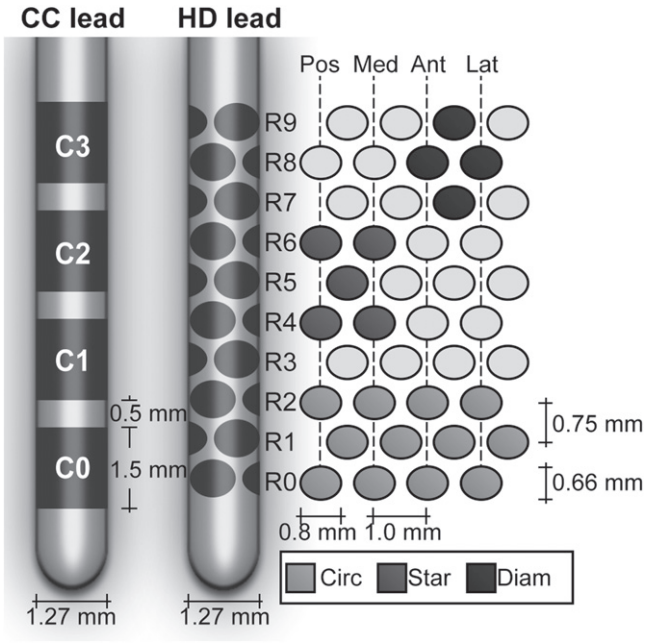

Figure 2. Representation of CC lead (left) and the HD lead with its schematic overview of the 40 contacts (right). Examples of the diam (ond) configuration in anterior–lateral direction, star configuration in posterior–medial direction, and circ(ular)-mode (R0–R2) of the HD lead are indicated in different gray scales.

generated by current stimulation, and was carried out in SCIRun v3.0.2 (University of Utah, Salt Lake City, US). The computed potential field formed the input into the neuron model, which is a multi-compartment neuron model programmed in NEURON 6.2 (Yale university, New Haven, US) [35]. The model consists of three neural populations in the subthalamic region, which are most likely activated by DBS. These neural populations are the STN projections cells, the efferent GPi fibers in the lenticular fasciculus, and the IC fibers. The STN and GPi axon trajectories were based on non-human primate cell tracings [36, 37], and the IC fiber trajectories were based on streamline tractography using the DTI dataset accompanying the brain atlas. Because of limited morphologic data of the axons of the neural populations, the variability between different axon models, and to enable consistent comparison between stimulation induced activation of the different neural populations, every axon was implemented with the same model parameters (5.7 μm axon diameter model [38]). Finally, SCIRun v3.0.2 was used for visualization of the complete model (figure 1).

DBS lead geometry

Either a CC lead or an HD lead (figure 2) was incorporated within the FEM model. The CC lead was based on the Medtronic 3389 electrode (Medtronic Inc., Minneapolis, US), which has a body diameter of 1.27 mm and carries four CCs (C0–C3). These contacts each have a length of 1.5 mm, a 6 mm^2 contact surface area, and an inter-electrode spacing of 0.5 mm. The HD lead was based on the Sapiens Steering Brain Stimulation lead design, which also has a diameter of 1.27 mm and carries 40 oval shaped electrode contacts. The 40 contacts are divided into ten rows (R0–R9) of four contacts, and each row is rotated by 45° from each other. Each oval shaped contact has a 0.42 mm^2 contact surface area, and contact center-to-center distances of 1 and 0.75 mm in the horizontal and vertical directions, respectively.

DBS lead location

For each simulation only one of the DBS leads was positioned in the STN. This DBS lead was positioned either at the center location, at a 1 mm off-center location, or at a 2 mm off-center location (figure 3). For the center location, the lead targeted the centroid of the STN: the second electrode contact from the tip (C1) of the CC lead was positioned in the center, the fourth row of electrode contacts from the tip (R3) of the HD lead was positioned in the center. At the off-center locations, the lead was linearly shifted 1 or 2 mm towards the IC, on the line between the centroid of the STN and the point given by the average location of the nearest axon segments of each IC fiber in the model. This resulted in a shift 0.46 mm posteriorly, 0.59 mm medially, and 0.66 mm ventrally with respect to the center location, per 1 mm displacement. For all three locations, the lead approached the target in an AC/PC-based coordinate system with a typical lead arc and collar angles of 20° and 100°, respectively (figure 3).

Stimulation protocols

Monopolar stimulation protocols were tested for different contact configurations and stimulation amplitudes. The stimulation signal was a biphasic charge-balanced stimulation pulse, i.e. a 100 μs rectangular waveform, with amplitudes ranging from −1 to −5 mA with a 0.5 mA step size, followed by a 5 ms period of low amplitude anodic stimulation. The outer boundary of the FEM model was used as reference for

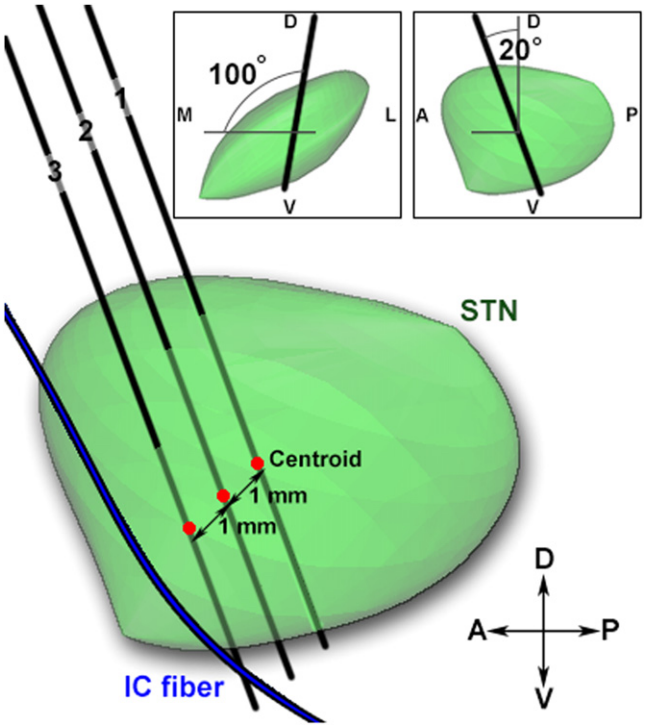

Figure 3. Representation of the DBS lead locations. The STN volume is shown in green, one IC fiber is shown in blue, and the three lead trajectories are shown by black lines. Trajectory 1 is the center location, trajectory 2 is the 1 mm off-center location, and trajectory 3 is the 2 mm off-center location. The top two views (left coronal, right sagittal) of the STN show the trajectory arc and collar angles of 20° and 100°, respectively, in an AC/PC-based coordinate system. The main (sagittal) view of the STN shows the shifts of the lead trajectory in the direction of the IC.

the return current. The stimulation signal was used for single source stimulation by evenly spreading the injected current over the selected electrode contact(s). The possible contact configurations varied per lead. For the CC lead, one of the four electrode contacts, C0–C3 (6.0 mm^2 activated electrode surface), was selected to simulate circular-mode stimulation (figure 2). For the HD lead, we distinguish two types of circular-mode stimulation and two types of steering-mode stimulations, i.e. HD circular 'mimic', HD circular 'free', HD star, and HD diamond (figure 2). For both HD circular modes, three adjacent rows, each with four electrode contacts, (5.0 mm^2 activated electrode surface) were selected for stimulation. In HD circular 'mimic' mode, we used the same stimulation pulse amplitude and similar vertical contacts height as the optimal CC configuration, i.e. R0–R2 for C0, R2–R4 for C1, R5–R7 for C2 and R7–R9 for C3. In HD circular 'free' mode, there were no constraints in the stimulation pulse amplitude and selection of the vertical contact height. In HD steering-mode, the electrode contacts were selected in either a star or diamond configuration. In the star configuration, five adjacent electrode contacts were selected in either medial, lateral, posterior, anterior, or any of the intermediate directions (2.1 mm^2 activated electrode surface). In the diamond configuration, four adjacent electrode contacts were selected in the medial, lateral, posterior, anterior, or any of the intermediate directions (1.7 mm^2 activated electrode surface). Stimulation in diamond configuration with −5 mA stimulation amplitudes results in the maximum charge density of 29 $\mu C\,cm^{-2}$, which is below the often recommended charge density limit of 30 $\mu C\,cm^{-2}$. For each stimulation mode, all possible directions and vertical positions of the configurations were simulated to find the optimal settings.

Activation of neural populations

The effect of the evoked potential field by each stimulation protocol (each amplitude and each contact configuration) was evaluated in the neuron part of the computational model. To quantify the differences between stimulation protocols we aimed to maximize the amount of activated STN cells without activating the IC fibers, but with allowing activation of efferent GPi fibers. A cell or axon is counted as activated when the stimulation pulse evoked at least one action potential that propagated to the end segment of the axon. The optimal stimulation protocol was defined as the configuration that activated the highest percentage of STN cells, without activating any IC fiber.

Statistical analysis

Fifteen datasets were created to compare the different stimulation configurations statistically. Five datasets were created with the leads at the center location and five datasets for each of the two off-center locations. For each dataset, the STN cell bodies were randomly distributed inside the STN, the GPi fibers were randomly distributed within a given boundary box dorsal to the STN, and the IC fibers were kept constant [32]. Differences were analyzed statistically, using a repeated measures ANOVA test with significance level of 0.05. When necessary, six Bonferroni corrected paired-sample t-tests were performed, i.e. the CC configuration with each of the four HD configurations, the two HD circular modes (free and mimic) with each other, and the two HD steering modes (star and diamond) with each other.

Results

In the model system, a population of 99 STN cells, a bundle of 99 GPi fibers, and a bundle of 199 IC fibers were placed in the subthalamic region. Each neuron with a cell segment located at the position of the DBS lead was removed from the model. For the 15 datasets, this resulted in neuron models including 182.3 ± 13.1 IC fibers, 99 GPi fibers, and 79.8 ± 4.3 STN cells.

Comparison of the CC and HD leads in circular-modes

We compared the circular-mode stimulation of the CC lead with the circular-mode stimulations of the HD lead, both with and without the mimicking constraints ('mimic' and 'free', respectively) (figure 4). The CC lead, with its optimal stimulation settings, was able to activate 56.6 ± 4.8% STN cells at center location, 31.4 ± 1.4% of STN cells at the 1 mm off-

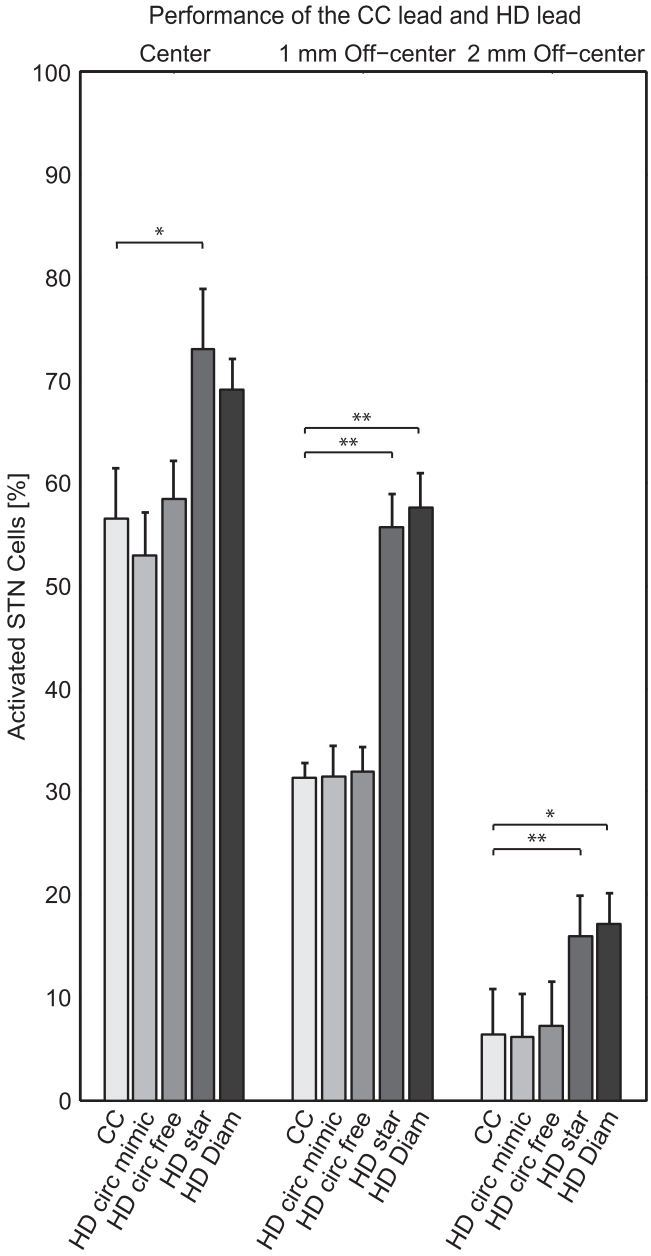

Figure 4. The performance of the five stimulation modes, i.e. the CC, HD circ(ular) mimic, HD circ(ular) free, HD star and HD diam(ond). Bars denote mean values with standard deviations of the percentage of activated STN cells after stimulation for the 5 datasets per lead location each with random distributions of the cells/fibers in the neural populations. Significant differences after Bonferroni correction for multiple comparisons ($n = 6$) are indicated with one asterisk ($p < 0.05$) or two asterisks ($p < 0.01$).

center location, and 6.4 ± 4.4% of STN cells at the 2 mm off-center location. The HD lead in circular 'mimic' mode was able to activate 53.0 ± 4.2% of STN cells at center location, 31.5 ± 3.0% cells at the 1 mm off-center location, and 6.2 ± 4.2% cells at the 2 mm off-center location. For all locations, there were no significant differences between the percentage of activation with the CC lead and with the HD lead in circular 'mimic' mode.

Ignoring the mimicking constraints, i.e. the circular 'free' model, resulted in a maximum activation of 58.5 ± 3.7% STN cells at center location, 31.9 ± 2.4% cells at the 1 mm off-center location, and 7.2 ± 4.3% cells at the 2 mm off-center location. In all cases, there were no significant differences between the CC lead and the HD lead, with regard to the number/percentage of activated STN cells and the overall currents that were used. The corresponding optimal stimulation pulse amplitudes for each lead location are presented in table 1.

Comparison of the CC and HD leads in steering-modes

Next, we compared the circular-mode stimulation of the CC lead with the HD lead in steering-mode (star and diamond configurations) (figure 4). The star configuration was able to activate 73.0 ± 5.9% of STN cells at the center location, 55.7 ± 3.2% cells at the 1 mm off-center location, and 16.0 ± 3.9% cells at the 2 off-center location. The percentage of activated STN cells by the HD lead in star steering mode was significantly larger at the center location ($p < 0.05/6$) as well as at the off-center locations ($p < 0.01/6$). The diamond configuration was able to activate 69.1 ± 2.9% of STN cells at the center location, 57.7 ± 3.3% cells at the 1 mm off-center location, and 17.1 ± 3.1% cells at the 2 mm off-center location. The percentage of activated STN cells by the HD lead in diamond steering mode was significantly larger at both off-center locations ($p < 0.01/6$ (1 mm) and $p < 0.05/6$ (2 mm)). There was no significant difference between the percentages of activated STN cells between the two types of steering configurations. The corresponding stimulation pulse amplitudes for each lead location are also included in table 1.

Finally, each stimulation mode individually activated significantly fewer STN cells at the 1 mm off-center location compared to the activation at center location ($p < 0.05$). However, there was no significant difference between the stimulation of the CC lead at center location and the HD lead stimulation in steering-mode at the 1 mm off-center location. In other words, while the displacement significantly decreased the percentage of STN cell activation of both leads according to our predefined criterion, the HD lead with the 1 mm displacement error was still able to activate a similar amount of STN cells as the CC lead located in the center of the STN (figure 5).

Discussion

In the current study, we used a computational model approach to investigate the stimulation effects of a new HD DBS lead design. The primary advantage of this HD lead is the ability to steer the stimulation field towards target areas and/or away from areas that cause side effects. However, the HD lead should also be able to mimic the conventional circular-mode stimulation. This requirement is important to ensure backwards compatibility with the currently used systems [22]. By stimulating with the HD lead at the same location and amplitude as the CC lead, the HD lead is able to activate a similar percentage of STN cells. Furthermore, the HD lead

Table 1. Stimulation effect of the CC lead and HD lead.

	Center		1 mm off-center		2 mm off-center	
	STN (%)	Amp (mA)	STN (%)	Amp (mA)	STN (%)	Amp (mA)
CC	56.6 ± 4.8	4.5 ± 0	31.4 ± 1.4	2.3 ± 0.45	6.4 ± 4.4	0.4 ± 0.22
HD circular 'mimic'	53.0 ± 4.2	4.5 ± 0	31.5 ± 3.0	2.3 ± 0.45	6.2 ± 4.2	0.4 ± 0.22
HD circular 'free'	58.5 ± 3.7	3.9 ± 0.9	31.9 ± 2.4	2.4 ± 0.22	7.2 ± 4.3	0.5 ± 0
HD star	73.0 ± 5.9	4.5 ± 0	55.7 ± 3.2	3.6 ± 0.82	16.0 ± 3.9	1 ± 0
HD diamond	69.1 ± 2.9	5 ± 0	57.7 ± 3.3	3.9 ± 0.22	17.1 ± 3.1	1.5 ± 0

Mean ± standard deviation of the percentage of activated STN cells with the corresponding stimulation amplitudes.

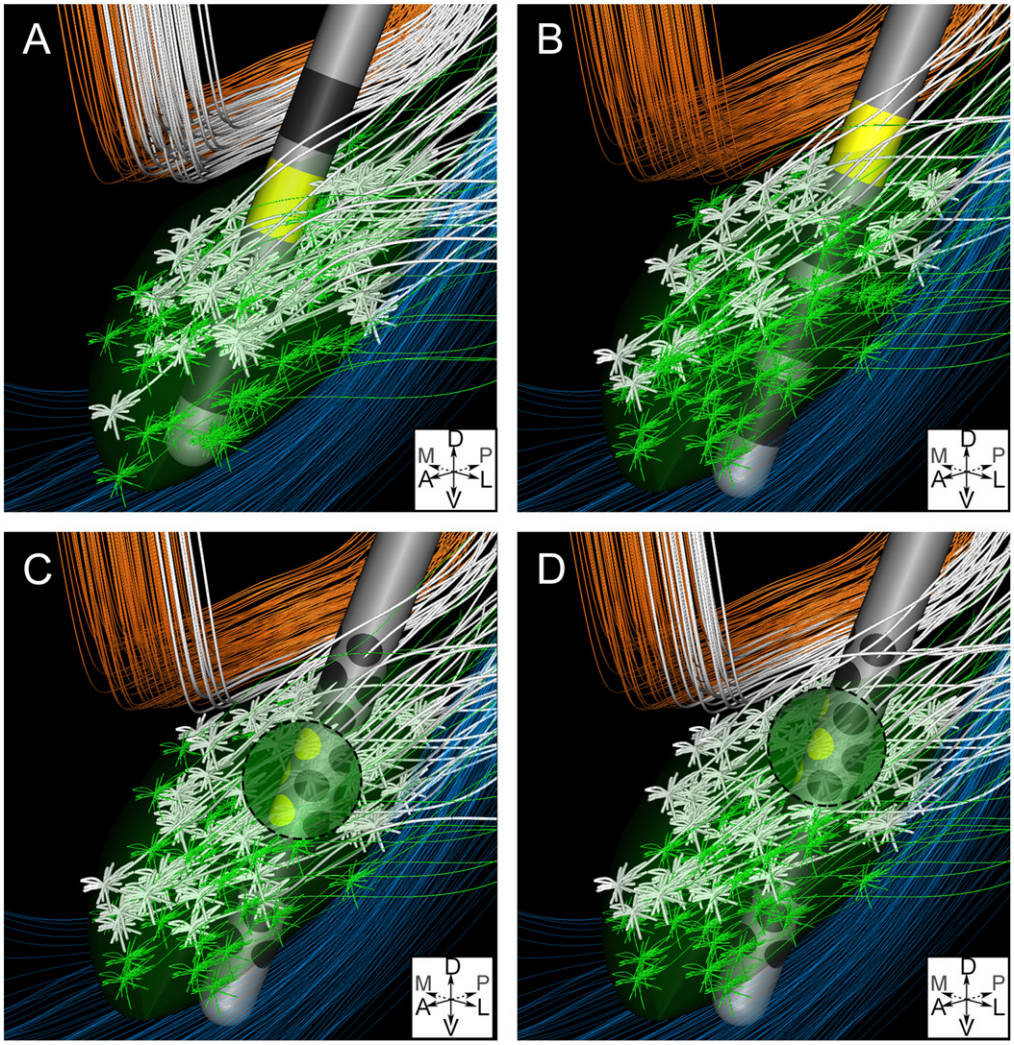

Figure 5. An example of the activation of STN cells illustrating the ability to compensate for a lead displacement error using the HD lead. The panels show the GPi efferent fibers in orange, STN cells in green, IC fibers in blue, and the STN cells in green. Cells and fibers that were activated by the stimulation pulse are displayed in white. (A) The optimal configuration of the CC lead at center location (4.5 mA, 53% stimulated STN cells). (B) The optimal configuration for the CC lead at the 1 mm off-center location (2.5 mA, 31% stimulated STN cells). (C) The optimal star steering configuration for the HD lead at the 1 mm off-center location (3 mA, 57% stimulated STN cells). (D) The optimal diamond steering configuration for the HD lead at off-center location (3,5 mA, 56% stimulated STN cells).

has more optional configurations than the CC lead. We studied all possible 'monopolar' circular-mode stimulation configurations with twelve electrode contacts in three adjacent rows. This resulted in eight different vertical positions with 0.75 mm resolution for the HD lead, against four heights with 1.5 mm resolution for the CC lead. Interestingly, the increased resolution in vertical position did not result in a significantly better performance of the HD lead in circular 'free' mode. A potential reason for this might be due to the use of three rows of smaller contacts in HD circular mode, when added together, this covers a slightly larger volume along the vertical direction as compared to a single CC contact. This reduces

some specificity of the HD lead. Additionally, the stimulating field in dorsal–ventral direction was only bound by the IC ventrally to the STN. Therefore, by adopting the criterion that IC fibers were not allowed to be activated, the shape of the electric field dorsal of the STN was less critical, and therefore the increased vertical spatial resolution of the HD lead had a minor influence.

When looking at the steering-mode stimulation, the results from the model clearly showed an increased activation by the HD lead compared to the stimulation with the CC lead. The most notable improvement was in the case where the lead was displaced 1 mm towards the IC. While the CC lead was on average only able to activate 31% of the STN cells, the HD lead activated on average 57% STN cells. This amount of activation for the HD lead was similar to the activation with the CC lead at center location. This suggests that the HD lead in steering mode, when displaced 1 mm towards the IC, is still able to generate the same neuron activation effect as the CC lead that is placed at the center of the STN. For the larger displacement of 2 mm, the HD lead in steering-mode stimulation was still able to activate significantly more STN cells than the CC lead. However, the percentages of activated STN cells were very low for all of the stimulation configurations at this location. By having the lead this close to the IC field steering cannot fully compensate for the lead displacement compared to the stimulation effects of the lead at center location.

We should note, however, that we only studied two types of steering-mode stimulation: star and diamond configuration. Other types of contact configurations as well as multipolar stimulation may further increase the performance of the HD lead in specific scenarios. Of course, the same applies for the CC lead. Chaturvedi *et al* [32] showed in a similar computational model that the CC lead in bipolar configuration with two independent sources performs significantly better than the lead in monopolar stimulation. However, allowing additional types of configurations for the HD lead will make it extremely complicated to manually find the optimal DBS settings. Therefore, we limited the configurations to two simple types of steering-modes. Both types used adjacent electrode contacts centered on certain heights and directions of the lead. The results showed no significant differences between the two configuration types. However, at center location there was no significant difference between the diamond configuration and the CC lead, while there was a significantly larger percentage of STN cells stimulated with the star steering configuration. Therefore, we prefer the star configuration for steering-mode stimulation. Also, the star configuration uses five instead of four electrode contacts, which results in a larger contact surface area, and therefore a lower current density per contact [39].

To quantify the stimulation effect we adopted the criterion that a maximum amount of activated STN cells is desired with DBS. Therefore, we searched, for each stimulation mode, for the highest percentage of activated STN cells and allowed activation of the GPi efferent fibers. Several studies [15, 40–42] show that patients with the best clinical outcome tend to have direct activation of axonal tissue dorsal to the STN compared to those who have stimulation confined within the STN. It has been suggested that adverse DBS effects are caused by the fact that the STN contains three functional modalities: motor, limbic and associative functions. Consequently, stimulation of the areas that are not concerned with motor function may result in adverse effects [18, 43]. Additionally, instead of maximizing the activation of motor STN cells it actually might be better to focus on the activation of passing GPi fibers [40], subpopulations of fibers within the IC [44], passing fibers of the substantia nigra [42], or cortical afferents to the STN [16]. Given all these uncertainties, we decided only to focus on maximization of the amount of the activated STN cells, which is conventionally considered as the main target for STN DBS. In principle it can be regarded as an example to show the steering effect of the HD lead on a plausible target.

We decided to focus on maximizing the activation effect, and not on minimizing energy consumption. The DBS battery is implanted under the skin below the clavicle and surgery is needed to replace it once it is depleted. Therefore, battery life is an important aspect in DBS therapy. Shaping the stimulation field to compensate for a lead displacement did demand higher stimulation amplitudes in our model simulations. However, because of the uncertainties with regard to the selection of target areas for optimal clinical effects, and inaccurate or lack of data on the resistivity of the contacts of the HD lead, a comparison of stimulation power for the different leads and configurations is at this point beyond the scope of our study.

Our model representation of the HD lead was included in a state of the art computational model of the subthalamic region that included many important and realistic details. The technical limitations of this computational model are well described in previous studies [15, 28, 31]. The limitations will have effect on the quantified percentage of activated STN cells. For example, all axons in this model have the same diameter of 5.7 μm and therefore the same dynamic properties and excitability [38]. In the human nervous system, long-distance connections typically tend to have larger axon diameters. Given this, the IC fibers probably have relatively large axon diameters, while the STN axon diameters are known to be smaller than 5.7 μm [45]. In this study, the size of the IC fibers was more important for the results, because the selection of the steering mode stimulation parameters was based on avoiding activation of these IC fibers. In general, larger diameter axons are more easily excitable than smaller diameter ones. Therefore, when using IC pathway activation as a proxy to avoid side-effects, it seemed logical to more accurately describe the IC axons with a larger diameter model. Finally, since our results focus on a comparison between the CC and HD leads in the same model, the limitations will influence both leads and therefore will have little impact on the comparison. The model already proved to be an adequate tool to study new stimulation paradigms for the CC lead [32]. In this study, we also showed that the model enables to explore new lead designs and prove the concepts of steering-mode stimulation.

In conclusion, we found that the concepts of steering the stimulation field with a HD lead design used in this study may be beneficial, and it allows to correct for lead displacement errors. We have demonstrated that even a simple steering-mode outperforms current state of the art systems. However, more research is needed on the stimulation of other therapeutic targets and side-effect regions. In the future this information can be incorporated into a patient specific model, based on the one used in this study, to help select the contact configuration with the best therapeutic window for each patient individually.

Acknowledgments

This work was supported by grants from the 'Toegepast Wetenschappelijk Instituut Voor Neuromodulatie' (TWIN). The authors would like to thank Hubert Martens and Mattias Åström (Medtronic Eindhoven Design Center) for providing background information and geometry of the HD lead.

References

[1] Breit S, Schulz J B and Benabid A L 2004 Deep brain stimulation *Cell Tissue Res.* **318** 275–88
[2] Benabid A L 2003 Deep brain stimulation for Parkinson's disease *Curr. Opin. Neurobiol.* **13** 696–706
[3] Machado A *et al* 2006 Deep brain stimulation for Parkinson's disease: surgical technique and perioperative management *Mov. Disorders* **21** (Suppl 14) S247–58
[4] Hamani C *et al* 2005 Bilateral subthalamic nucleus stimulation for Parkinson's disease: a systematic review of the clinical literature *Neurosurgery* **56** 1313–21 discussion 1321–4
[5] Krack P *et al* 2003 Five-year follow-up of bilateral stimulation of the subthalamic nucleus in advanced Parkinson's disease *New. Engl. J. Med.* **349** 1925–34
[6] Odekerken V J *et al* 2013 Subthalamic nucleus versus globus pallidus bilateral deep brain stimulation for advanced Parkinson's disease (NSTAPS study): a randomised controlled trial *Lancet Neurology* **12** 37–44
[7] Hamani C *et al* 2004 The subthalamic nucleus in the context of movement disorders *Brain* **127** 4–20
[8] Hamel W *et al* 2003 Deep brain stimulation of the subthalamic nucleus in Parkinson's disease: evaluation of active electrode contacts *J. Neurology Neurosurgery Psychiatry* **74** 1036–46
[9] Okun M S *et al* 2005 Management of referred deep brain stimulation failures: a retrospective analysis from 2 movement disorders centers *Arch. Neurology* **62** 1250–5
[10] Fitzpatrick J M *et al* 2005 Accuracy of customized miniature stereotactic platforms *Stereotact. Funct. Neurosurgery* **83** 25–31
[11] Zylka W, Sabczynski J and Schmitz G 1999 A Gaussian approach for the calculation of the accuracy of stereotactic frame systems *Med. Phys.* **26** 381–91
[12] van den Munckhof P *et al* 2010 Postoperative curving and upward displacement of deep brain stimulation electrodes caused by brain shift *Neurosurgery* **67** 49–53 discussion 53-4
[13] Contarino M F *et al* 2013 Postoperative displacement of deep brain stimulation electrodes related to lead-anchoring technique *Neurosurgery* **73** 681–8
[14] McIntyre C C *et al* 2004 Electric field and stimulating influence generated by deep brain stimulation of the subthalamic nucleus *Clin. Neurophysiol.* **115** 589–95
[15] Miocinovic S *et al* 2006 Computational analysis of subthalamic nucleus and lenticular fasciculus activation during therapeutic deep brain stimulation *J. Neurophysiol.* **96** 1569–80
[16] Li S *et al* 2007 Resonant antidromic cortical circuit activation as a consequence of high-frequency subthalamic deep-brain stimulation *J. Neurophysiol.* **98** 3525–37
[17] Frankemolle A M *et al* 2010 Reversing cognitive-motor impairments in Parkinson's disease patients using a computational modelling approach to deep brain stimulation programming *Brain* **133** 746–61
[18] Temel Y *et al* 2005 The functional role of the subthalamic nucleus in cognitive and limbic circuits *Prog. Neurobiol.* **76** 393–413
[19] Funkiewiez A *et al* 2003 Acute psychotropic effects of bilateral subthalamic nucleus stimulation and levodopa in Parkinson's disease *Mov. Disorders* **18** 524–30
[20] Krack P *et al* 2002 Postoperative management of subthalamic nucleus stimulation for Parkinson's disease *Mov. Disorders* **17** (Suppl 3) S188–97
[21] Tamma F *et al* 2002 Anatomo-clinical correlation of intraoperative stimulation-induced side-effects during HF-DBS of the subthalamic nucleus *Neurological Sci.* **23** (Suppl 2) S109–10
[22] Martens H C *et al* 2011 Spatial steering of deep brain stimulation volumes using a novel lead design *Clin. Neurophysiol.* **122** 558–66
[23] Willsie A and Dorval A D 2013 Charge steering in a novel DBS electrode may accommodate surgical targeting errors *Proc. of the 6th Int. IEEE/EMBS Conf. on Neural Engineering (NER)*
[24] Contarino M F *et al* 2014 Directional steering: a novel approach to deep brain stimulation *Neurology* **83** 1163–9
[25] Keane M *et al* 2012 Improved spatial targeting with directionally segmented deep brain stimulation leads for treating essential tremor *J Neural Eng.* **9** 046005
[26] Pollo C *et al* 2014 Directional deep brain stimulation: an intraoperative double-blind pilot study *Brain* **137** 2015–26
[27] Astrom M, Lemaire J J and Wardell K 2012 Influence of heterogeneous and anisotropic tissue conductivity on electric field distribution in deep brain stimulation *Med. Biol. Eng. Comput.* **50** 23–32
[28] Chaturvedi A *et al* 2010 Patient-specific models of deep brain stimulation: influence of field model complexity on neural activation predictions *Brain Stimul.* **3** 65–7
[29] Butson C R and McIntyre C C 2005 Tissue and electrode capacitance reduce neural activation volumes during deep brain stimulation *Clin. Neurophysiol.* **116** 2490–500
[30] Butson C R and McIntyre C C 2006 Role of electrode design on the volume of tissue activated during deep brain stimulation *J. Neural Eng.* **3** 1–8
[31] Butson C R *et al* 2007 Patient-specific analysis of the volume of tissue activated during deep brain stimulation *Neuroimage* **34** 661–70
[32] Chaturvedi A, Foutz T J and McIntyre C C 2012 Current steering to activate targeted neural pathways during deep brain stimulation of the subthalamic region *Brain Stimul.* **5** 369–77
[33] Wakana S *et al* 2004 Fiber tract-based atlas of human white matter anatomy *Radiology* **230** 77–87
[34] Tuch D S *et al* 2001 Conductivity tensor mapping of the human brain using diffusion tensor MRI *Proc. Natl Acad. Sci. USA* **98** 11697–701
[35] Hines M L and Carnevale N T 1997 The neuron simulation environment *Neural Comput.* **9** 1179–209

[36] Sato F *et al* 2000 Axonal branching pattern of neurons of the subthalamic nucleus in primates *J. Comp. Neurology* **424** 142–52
[37] Parent M and Parent A 2004 The pallidofugal motor fiber system in primates *Parkinsonism Relat. Disorders* **10** 203–11
[38] McIntyre C C, Richardson A G and Grill W M 2002 Modeling the excitability of mammalian nerve fibers: influence of afterpotentials on the recovery cycle *J. Neurophysiol.* **87** 995–1006
[39] Shannon R V 1992 A model of safe levels for electrical-stimulation *IEEE Trans. Biomed. Eng.* **39** 424–6
[40] Maks C B *et al* 2009 Deep brain stimulation activation volumes and their association with neurophysiological mapping and therapeutic outcomes *J. Neurology Neurosurgery Psychiatry* **80** 659–66
[41] Yelnik J *et al* 2003 Localization of stimulating electrodes in patients with Parkinson disease by using a three-dimensional atlas-magnetic resonance imaging coregistration method *J. Neurosurgery* **99** 89–99
[42] Herzog J *et al* 2004 Most effective stimulation site in subthalamic deep brain stimulation for Parkinson's disease *Mov. Disorders* **19** 1050–4
[43] Janssen M L *et al* 2012 Subthalamic neuronal responses to cortical stimulation *Mov. Disorders* **27** 435–8
[44] Xu W *et al* 2011 Dissociation of motor symptoms during deep brain stimulation of the subthalamic nucleus in the region of the internal capsule *Exp. Neurology* **228** 294–7
[45] Mathai A, Wichmann T and Smith Y 2013 More than meets the eye-myelinated axons crowd the subthalamic nucleus *Mov. Disorders* **28** 1811–5